UCRL-18380

cy. 2

RECEIVED
LAWRENCE
RADIATION LABORATORY

SEP 19 1968

LIBRARY AND
DOCUMENTS SECTION

University of California

Ernest O. Lawrence Radiation Laboratory

TWO-WEEK LOAN COPY

This is a Library Circulating Copy which may be borrowed for two weeks. For a personal retention copy, call Tech. Info. Division, Ext. 5545

DYNAMICS OF THE REACTIONS OF N_2^+ WITH CH_4 AND CD_4

E. A. Gislason, Bruce H. Mahan, Chi-wing Tsao, and Arthur Werner

July 1968

UCRL-18380
cy. 2

Berkeley, California

DISCLAIMER

This document was prepared as an account of work sponsored by the United States Government. While this document is believed to contain correct information, neither the United States Government nor any agency thereof, nor the Regents of the University of California, nor any of their employees, makes any warranty, express or implied, or assumes any legal responsibility for the accuracy, completeness, or usefulness of any information, apparatus, product, or process disclosed, or represents that its use would not infringe privately owned rights. Reference herein to any specific commercial product, process, or service by its trade name, trademark, manufacturer, or otherwise, does not necessarily constitute or imply its endorsement, recommendation, or favoring by the United States Government or any agency thereof, or the Regents of the University of California. The views and opinions of authors expressed herein do not necessarily state or reflect those of the United States Government or any agency thereof or the Regents of the University of California.

Submitted to the Journal of Chemical Physics

UCRL-18380
Preprint

UNIVERSITY OF CALIFORNIA

Lawrence Radiation Laboratory
Berkeley, California

AEC Contract No. W-7405-eng-48

DYNAMICS OF THE REACTIONS OF N_2^+ WITH CH_4 AND CD_4

E. A. Gislason, Bruce H. Mahan, Chi-wing Tsao,

and Arthur Werner

July, 1968

Dynamics of the Reactions of N_2^+ With CH_4 and CD_4

E. A. Gislason, Bruce H. Mahan, Chi-wing Tsao,
and Arthur Werner

Inorganic Materials Research Division of the Lawrence
Radiation Laboratory and Department of Chemistry,
University of California, Berkeley, California.

ABSTRACT

Product velocity vector distributions have been determined for the reactive and nonreactive scattering of N_2^+ by CH_4, CD_4, and Ne. In the most probable reactive events, N_2H^+ and N_2D^+ are scattered forward at almost exactly the velocity calculated from the ideal stripping model. At the higher projectile energies, the internal excitation of CH_3 even for zero angle scattering is significant, and product internal excitation increases with increasing angle. A large isotope effect favoring abstraction of H over D was found. The nonreactive scattering showed the occurrence of highly inelastic collisions, even for small angle scattering, and a feature which may be due to the collisional electronic excitation of CH_4 or of N_2^+ was discovered.

Many of the details of the dynamics of gaseous ion-molecule reactions can be deduced from measurements of the energy and angular distributions of the ionic products and scattered reactants. The first investigations[1-4] in this area have been largely concentrated on the reaction of N_2^+ with the isotopic hydrogen molecules, because of its simplicity, large cross section, and a kinematic factor favorable for detection of the products. At relative kinetic energies above 3 eV, some of the prominent features of the N_2H^+ velocity vector distributions are direct consequences of the fact that the other (atomic) product cannot take up energy as internal excitation. Therefore, it seems of interest to examine a similar reaction in which both products were polyatomic in order to see if the presence of extra internal degrees of freedom significantly affects the partitioning of energy between internal and translational modes of the products. In this paper we report and discuss our measurements of the reactive and nonreactive scattering of N_2^+ by CH_4, CD_4, and Ne.

EXPERIMENTAL

The apparatus employed in this work is the same as was used in our investigation of the N_2^+-H_2 reaction.[3,4] Briefly, it consists of a magnetic mass spectrometer for preparation of the primary ion beam of known energy, a scattering cell containing the target gas, a 90° spherical electrostatic energy analyzer, a quadrupole mass spectrometer, and an ion counter. The energy distribution of ions at various laboratory angles

from the primary beam was determined by sweeping the electrostatic energy analyzer, and the angular distribution of ions of fixed energy was measured by rotating the entire detection train with respect to the primary ion beam. Further details of the apparatus and procedure can be found in our earlier publications.[3,4] In the present experiments, momentum analysis of the projectile beam was performed at an energy of 32 eV, which produced a beam energy spread of 0.96 eV FWHM.

RESULTS AND DISCUSSION

Figure 1 shows a velocity vector diagram for 25 eV (laboratory) N_2^+ impinging on a CH_4 target. The small circle about the laboratory velocity origin indicates the locus of the rms thermal velocity vectors of the methane molecule. The assumption of a stationary target for 25 eV and higher projectile energies seems quite well justified.

The region of velocity space where the ionic product of the reaction

$$N_2^+ + CH_4 \rightarrow N_2H^+ + CH_3 \qquad (1)$$

can appear is limited by the possible extreme values of Q, the difference between final and initial relative kinetic energies. Since for ground state reactants

$$Q = - \Delta E_o^o - U$$

where ΔE_o^o is the energy change of the reaction, and U is the internal excitation of the product molecules, the values of Q consistent with reaction (1) are given by

$$-\Delta E_o^o - U_{max} \leq Q \leq -\Delta E_o^o$$

or

$$-\Delta E_o^o - D(N_2 - H^+) - D(CH_2 - H) \leq Q \leq -\Delta E_o^o \qquad (2)$$

That is, for products in their electronic ground states, the final internal excitation energy U must not exceed the sum of the smallest dissociation energies of N_2H^+ and CH_3. Equation (2) can also be expressed as

$$-2.5 - D(CH_2 - H) \leq Q \leq -\Delta E_o^o$$

which is based on a value of 4.5 eV for the first bond dissociation energy of methane. Thus there is a lower limit for the Q of reaction (1) of - 7.2 eV if $D(CH_2\text{-}H)$ is taken as 4.7 eV.[5] Any N_2H^+ observed in regions of velocity space that correspond to smaller values of Q must come from collisions in which the methyl group is fragmented or electronically excited.

The upper limit for Q is uncertain since ΔE_o^o or equivalently $D(N_2\text{-}H^+)$ is not known exactly. We have previously estimated for $D(N_2\text{-}H^+)$ a lower limit of 2.5 eV and an upper limit of 3.5 eV. The latter corresponds to a value of -1 eV for ΔE_o^o. In the contour maps of scattered particle intensity as a function of speed and angle in the center of mass system which will be presented, the loci of velocities of N_2^+, N_2H^+, or N_2D^+ which correspond to certain critical values of Q appear as circles about the origin.

In our earlier investigation of the N_2^+-H_2 reaction, the large ratio of projectile to target mass insured that all scattered particles were confined to a very small range of laboratory angles and speeds, regardless of their center of mass scattering angle. Thanks to this kinematic concentration, we were able to determine the complete center of mass velocity vector distribution of products. In the N_2^+-CH_4 system, however, the masses of projectile and target are more nearly comparable, and therefore, the scattered products can be spread out over a much larger range of laboratory scattering angles and speeds. It is possible, therefore, that products scattered through large center of mass angles will not be detected for two reasons. First, large angle scattering, intrinsically weak because it comes from small impact parameter collisions, would be spread very thinly through a large region in velocity space, and the counting rate in the velocity space volume of the detector could easily be too small to be seen above background. Second, the ions scattered through center of mass angles near 180° are moving with quite small velocities in the laboratory, as is clear from Fig. 1. Since the transmission of our detection train falls for ions of less than 10 eV energy, many of the particles scattered through large angles might not reach the detector. It was important, therefore, to perform an experiment which would indicate the sensitivity of the apparatus to products scattered through large angles. To this end, we studied the scattering of N_2^+ by Ne.

Figure 2 shows an intensity contour map in the center of mass coordinate system of N_2^+ scattered by Ne at a relative energy of 31.5 eV. In this contour map and all others we follow our usual procedure[3] of plotting the counts per second per unit velocity space volume, normalized to scattering gas pressure, beam strength, and scattering volume. As we have pointed out,[4] this quantity is the same in the center of mass and laboratory coordinate systems. The scattering at small angles is largely elastic, since it falls on or near the Q = 0 circle. At large angles the scattering is increasingly inelastic as is indicated by the noncircular dashed line which runs through the peak scattered intensity at each center of mass angle. The magnitude of the energy loss suggests rotational and vibrational excitation of N_2^+ is occurring, and the low-lying (1.12 eV) A $^2\pi$ state of N_2^+ may also be excited. The scattered signal becomes difficult to detect at center of mass angles of approximately ± 60°. At these angles, however, the scattered N_2^+ still has approximately 50 eV laboratory translational energy, which is certainly high enough to assure efficient transmission and detection. Thus our failure to detect N_2^+ scattered from Ne through angles greater than ± 60° has a simple interpretation. Even for this case, in which the scattering is fairly well confined to a spherical shell in velocity space, with our present combination of ion beam intensity, scattering gas pressure, and detector resolution, the back-scattered ions are spread so thinly in velocity space that they cannot be detected. Consequently, for nonreactive or reactive scattering of N_2^+ by

CH_4, the great number of possible final internal states will tend to spread the products even more thinly in velocity space, and we cannot expect to observe the scattered particles at large center of mass angles.

Figure 3 shows the N_2H^+ intensity distribution from the N_2^+-CH_4 reaction at 25 eV laboratory, or 9.1 eV relative energy. As expected, the detectable scattering was confined to rather small angles in the center of mass system. The maximum intensity occurs very close to the velocity (indicated by a cross) calculated using the ideal stripping model. The N_2^+ beam profile at 20% maximum intensity and the similar one for N_2H^+ intercept only $\pm$ 3.5° and $\pm$ 6.5° in the center of mass system, which again indicates that very little impulse is imparted to the methyl radical in most reactive events.

It is clear from Fig. 3 that the scattered products lie at velocities which correspond to Q values less than + 1 eV. This shows that the 1.0 eV exothermicity of the reaction appears as internal energy of the products, and not as relative translational energy. At the larger scattering angles, the most probable value of Q tends to be slightly more negative than at smaller angles. It seems reasonable that in the smaller impact parameter collisions which lead to larger angle scattering, the methyl radical might interact with projectile more strongly, and thereby acquire larger internal excitation. The dependence of Q on scattering angle displayed here is opposite to that observed for the N_2^+-H_2 system.[3,4] In this latter case, the

N_2H^+ product scattered through small angles is excited almost to its dissociation limit, while at large scattering angles the product internal excitation is approximately 0.7 eV smaller, and Q correspondingly less negative. Apparently in this case the strong interaction of the departing ion N_2H^+ with an atomic neutral having no accessible internal modes produces a lowering of the product internal excitation at large scattering angles, whereas in the N_2^+-CH_4 collisions the stronger interaction between N_2H^+ and CH_3 tends to leave internal energy in the methyl radical.

Figure 4 shows the nonreactive scattering of N_2^+ by CH_4 at 9.1 eV relative energy. Essentially all the observed scattering is slightly inelastic, with Q = -0.8 eV. The separate closure of the two wings of the distribution and the absence of intensity in the region of the unscattered beam results from computing the intensity from I_{obs}-I_{beam}, where I_{beam} is the intensity due to the beam with no scattering gas, and I_{obs} is the signal with gas in the cell. The introduction of scattering gas of course gives a net attenuation of the nonreactive signal in the center of the beam. Hence at this point I_{obs}-I_{beam} is negative, and no information is obtained. Away from the beam center, when I_{beam} has fallen to 10-20% of its peak value, the nonreactively scattered signal I_{obs} usually is much larger than I_{beam}, and scattering information can be obtained. However, if there is a large reactive cross section, then the nonreactive signal I_{obs} will be attenuated, and thus I_{obs}-I_{beam} may remain negative out to center of mass angles of

approximately 5°-10°. This is the case for the N_2^+-CH_4 system, whose reactive cross section is large at low energies, and is the reason why the intensity contours of Fig. 2 close at approximately 10°.

At any particular scattering angle greater than 10°, the reactive and nonreactive scattering are distributed in speed differently, but have approximately the same intensity. The nonreactive scattering is confined to a relatively small range of Q values, and the distribution does not broaden appreciably in speed as the scattering angle increases. Consequently, if chemical reaction were not occurring, we should expect to observe the nonreactive scattering to angles of approximately 60°, as in the N_2^+-Ne system. Since no nonreactive scattering is detected beyond 30°, we can conclude that the various reactive processes must also attentuate the nonreactive signal for the smaller impact parameter collisions that would lead to larger angle nonreactive scattering.

Figure 5 shows the distribution of N_2D^+ from the N_2^+-CD_4 reaction at 10.4 eV relative energy. The peak product intensity is almost a factor of ten smaller than that found for the N_2^+-CH_4 system at the comparable relative energy. This very large isotope effect for small angle scattering was also observed for the N_2^+-HD system,[4] and is evidently characteristic of the stripping mechanism. The maximum intensity of N_2D^+ occurs very near to the product velocity calculated from the ideal stripping model, which is indicated by a cross in Fig. 5. The product distribution is sharply peaked in angle, with the 20% of maximum

intensity profile intercepting only ± 7° in the center of mass system, just as was true for N_2H^+ from CH_4. Again, there is no evidence of strong forward recoil, and consequently the exothermicity of reaction appears as product internal excitation.

The nonreactive scattering of N_2^+ by CD_4 at 12.5 eV relative energy, shown in Fig. 6, is somewhat similar to the corresponding N_2^+-CH_4 data. The scattering is slightly inelastic, and is confined to angles smaller than ± 30°. The intensity contours do not close at the small angles shown in Fig. 6 because the background beam attenuation due to reactive scattering is much smaller than for the N_2^+-CH_4 system. The intensity of scattered N_2^+ at any fixed angle is greater from CD_4 than from CH_4 at comparable relative energies. This also must be a consequence of the smaller reaction cross section observed for CD_4. Again, the disappearance of nonreactive scattering at angles as small as 30° indicates that small impact parameter collisions lead to charge transfer or chemical reaction with products spread throughout velocity space.

The reactive and nonreactive scattering of the N_2^+-CD_4 system at 50 eV laboratory (20.8 eV relative) energy were also mapped, but are not shown here. The N_2D^+ product had a maximum intensity almost exactly 0.1 of that observed in the experiment at 10.4 eV relative energy. In all other respects the product distribution resembled what was found at 10.4 eV. The intensity maximum fell almost exactly at the ideal stripping velocity, the 20% intensity contour fell within ± 8°, and virtually all detected product occurred at Q values between -1.8 and -4.5 eV.

The value of Q at the intensity maximum was -3.0 eV. If all the product internal excitation was present in N_2D^+, the most negative value of Q consistent with a stable N_2D^+ would be -2.5 eV. Since we observed the peak intensity of N_2D^+ was associated with a Q of -3.0 eV, there must be at least 0.5 eV internal excitation energy in the CD_3 group formed by the most probable reactive process.

The nonreactive scattering at 20.8 eV was qualitatively similar to that observed at 10.4 eV, except that the Q values are more negative, which indicates that the higher energy collisions are more inelastic. A map of the intensity of N_2H^+ from the N_2^+-CH_4 reaction at 27.3 eV relative energy was also prepared, and has been published elsewhere.[6]

The distribution of N_2H^+ from the N_2^+-CH_4 reaction carried out with a projectile energy of 110 eV or a relative energy of 40 eV is shown in Fig. 7. The intensity peak lies almost exactly at the ideal stripping velocity which is marked by a cross. The corresponding Q value is -3.3 eV, which by the argument given above indicates that the methyl radical formed in the most probable type of collision must have at least 0.8 eV internal excitation energy. From the intensity contours it is clear that in a substantial fraction of the observable reactive collisions, much larger amounts of internal energy are transferred to the methyl group. Appreciable intensity appears on the Q = -7.2 eV circle, at which the minimum energy in the methyl group is equal to its bond dissociation energy.

Unless this energy is present as electronic excitation of CH_3, the reaction which produces N_2H^+ associated with Q values more negative than -7.2 eV must be

$$N_2^+ + CH_4 \rightarrow N_2H^+ + CH_2 + H$$

Some intensity is observed even at the Q = -11.7 eV circle, and product formed at this velocity must come from

$$N_2^+ + CH_4 \rightarrow N_2H^+ + CH + 2H$$

unless the excess internal energy is taken up as electronic excitation of CH_2.

Figure 8 shows the distribution of 110 eV N_2^+ projectiles scattered by CH_4. Most of the observed scattering appears to be inelastic with a relative energy loss of 4.4 eV or less. There is, however, appreciable scattering in which the inelastic loss is much greater. The Q values of -4.4, -13.6, and -17.1, indicated by circles in Fig. 8, correspond to excitation energies sufficient to cause methane to dissociate into one, three, and four hydrogen atoms, respectively. The Q value for dissociation to two hydrogen atoms is -9.1 eV, and is located quite close to the Q = -8.2 eV circle in Fig. 8. Of course, some of the internal energy may appear as excitation of N_2^+, or as electronic excitation of some of the hydrocarbon dissociation fragments, so that the dissociation of methane may not be complete even for Q values more negative than -17.1 eV. Thus, because of the large number of available final states, it is not possible to specify the neutral products of these very

inelastic collisions. The data are significant in that they show that even for rather small scattering angles, very inelastic scattering can occur. Consequently we can expect that the small impact parameter collisions that lead to the unobservable large angle scattering will be even more inelastic, and will produce high levels of electronic excitation and or dissociation.

One other feature of Fig. 8 requires comment. There is a small peak in the intensity distribution at 0° and Q = -8.2 eV. This peak also appears with the same intensity and Q value when CD_4 is the scattering gas, and is also detectable in the scattering of N_2^+ from CH_4 at 75 eV projectile energy. The location of the peak at 0°, and its quite narrow profile make it likely that it arises from an electronic excitation process. The first allowed electronic transition of CH_4 has a threshold at 8.5 eV. The C $^2\Sigma_u^+$ state of N_2^+ lies 8.0 eV above the ground state, and thus either electronic excitation of N_2^+ or CH_4 could be responsible for the observed peak. Figure 2 shows that the peak is not present when N_2^+ is scattered by Ne, and this suggests that in N_2^+-CH_4 collisions it is the CH_4 which is being excited. On the other hand, we have observed rather weak excitation of the 8.0 eV level of N_2^+ in collisions with Ar at comparable relative energies. The process which occurs in the N_2^+-CH_4 system, therefore, must remain unclear until spectroscopic investigations can show whether or not the C $^2\Sigma_u^+$ state of N_2^+ is excited in these collisions.

Table I summarizes some of the numerical results which we have derived from our experiments. As we saw from the maps, the product velocity is in all cases very close to that calculated from the ideal stripping model. The product to projectile laboratory velocity ratio v/v_o is, according to the model, simply $M/(M+m)$, where M is the mass of N_2^+, and m is the mass of the transferred H or D atom. For the transfer of H or D, v/v_o is 0.966 and 0.933, respectively. The velocity ratios in Table I are all very close to these predicted values.

The close agreement over a wide energy range between observed values of v/v_o and those predicted from the ideal stripping model found in the N_2^+-CH_4 system is in contrast to the results for the N_2^+-H_2, D_2, and HD system. In the latter case, the observed[3,4] values of v/v_o were greater than those predicted from the model, and became more so as the projectile energy increased. There is a simple explanation for the difference. According to the stripping model, the internal excitation energy of the product U is the sum of the exothermicity of reaction $-\Delta E_o^o$, and E_a^o, the energy of the projectile relative to the atom it abstracts:

$$U = -\Delta E_o^o + E_a^o$$

For the reaction of N_2^+ with the isotopic hydrogen molecules, all the product internal excitation must be present in N_2H^+, and since the ion will not be stable if U exceeds its smallest dissociation energy, there is a natural upper limit[4] of

E_a^o = 2.5 eV for operation of the ideal stripping model. For N_2^+-CH_4 collisions this limitation of the ideal stripping model to low energies does not exist, since the internal excitation energy U may enter the methyl group and allow the N_2H^+ to stay below its dissociation limit and still move with the ideal stripping velocity. It is questionable whether one should continue to describe such very high energy collisions as "ideal" stripping processes, for although the value of the velocity ratio v/v_o implies a weak interaction between the projectile N_2^+ and the spectator CH_3, the amount of energy that must necessarily be transferred to the internal modes of CH_3 suggests that the interaction is not weak.

The quantity that appears in the intensity contour maps is $\bar{I}(\theta,u)$, the normalized intensity per unit velocity space volume, averaged over the detector. From this quantity, absolute differential cross sections $I(\theta)$ and total cross sections σ were calculated using the relations

$$I(\theta) = \int_0^\infty \bar{I}(\theta,u)\ u^2 du \tag{3}$$

$$\sigma = 2\pi \int_0^\pi I(\theta)\ \sin\theta\ d\theta \tag{4}$$

and the results are given in Table I and Figs. 9 and 10. Although the transmission factor of our detector system has been found to be constant over a wide range of energies, the actual value of the factor is difficult to determine accurately. Consequently we have scaled all of our results for N_2^+ reactions

to the total reaction cross section for N_2^+-D_2 at 11.2 eV relative energy which was measured by Turner et al.[7] Such calculations and the normalization were discussed in our earlier work.[4] We estimate that the uncertainty in the total cross sections due to experimental uncertainties and the normalization factor is ± 25%. The uncertainties in the absolute differential cross sections are at least this large.

The reduced differential cross sections $I(\theta)/I(\theta=0°)$ for the reactive scattering are shown in Fig. 9, and the values of $I(\theta=0°)$ are given in Table I. For the N_2^+-CH_4 system, the angular distribution $I(\theta)/I(0)$ becomes markedly broader with increasing projectile energy. The data in Table I show that at $\theta = 0°$ the intensity falls rapidly as the projectile energy increases. The intensity maps here and in Ref. 6 show that at the higher energies, very inelastic reactive processes occur, particularly at large angles. The combination of these effects produces the broadening in $I(\theta)/I(0)$. Evidently as projectile energy increases, the contributions of the grazing collisions to the reaction cross section are lost, and the more violent smaller impact parameter collisions increase in relative importance.

The rather limited data on reactive collisions for the CD_4 system do not show the broadening of $I(\theta)/I(0)$ at the higher energy. The larger momentum changes associated with large angle reactive scattering of the heavier isotopic product are apparently not favored, just as one might expect from the Born approximation, for example.

The experimental values of the total reaction cross section are shown in Fig. 10 along with the results for the N_2^+-H_2, D_2, and HD systems,[4] for comparison. These total cross sections are plotted as functions of E_a^o, since for the molecular hydrogen systems at least, the cross section for abstraction of H and D are very nearly equal at the same value of E_a^o. The two isotopic methanes have, however, quite different total cross sections even at the same value of E_a^o. The difference between the molecular hydrogen systems on one hand, and the methane systems on the other, may be at least partially related to the availability of internal modes in CH_3 but not the hydrogen atom. The large high energy isotope effect for forward scattering and in the total cross section of the molecular hydrogen system has been attributed to the difficulty of product stabilization[4] through forward recoil. The observation that the cross section for forming N_2H^+ and N_2D^+ from isotopic molecular hydrogens is the same at the same E_a^o is attributed to the fact that the incipient internal excitation energy of an ion formed by stripping is $-\Delta E_o^o + E_a^o$, which is the same for various isotopes at a given E_a^o. Thus the stabilization problem is the same for both isotopes at the same E_a^o. In the methane system, forward recoil is not necessary to stabilize the product ion, and the significance of E_a^o must be diminished. Thus it is not too surprising that the cross sections for the isotopic methanes are not the same at a given E_a^o.

It is obvious that the total reaction cross sections for the N_2^+-methane systems are smaller than those for the N_2^+-hydrogen systems. This is perhaps surprising in view of the virtually identical energetics of these reactions, and the product stabilization problem that exists in the N_2^+-hydrogen system. It may be, however, that the undetected products scattered through large angles in N_2^+-CH_4 collisions may account for a significant fraction of the difference in total cross sections.

It has been pointed out that the intensity observed at very negative Q values in the higher energy experiments may represent collisions in which the methyl radical is fragmented or electronically excited. In order to display in a more quantitative manner the increasing importance of such highly endothermic collisions, we computed partial differential and total cross sections which include only intensity that lies at $Q \geq -4.7$ eV. This cut off value of -4.7 eV for Q was chosen somewhat arbitrarily, although $Q > -4.7$ eV does correspond to a region of velocity space in which excitation of CH_3 to its lowest known electronic level is not possible. The results are shown in Fig. 10 and Table I, and it is clear that highly endothermic collisions constitute an important fraction of the reactive processes at high collision energies.

Although the data of Fig. 2 were intended primarily as a test of the apparatus sensitivity, a comment concerning their interpretation is in order. We have computed differential cross sections for the N_2^+ - Ne scattering using Eq. 3 for the

region between $\theta = 20°$ and $50°$ at $5°$ intervals. Although $I(\theta)$ falls off rapidly with increasing angle, we found that

$$\theta \sin\theta \, I(\theta) = 0.76 \text{ Å}^2/\text{sr}$$

is a very good approximation at all angles (stnd. dev. = 0.06 Å^2). Since the relative energy in the experiment was fairly high (31.5 eV) and the observed intensity fell outside the very small angle region, the scattering is clearly from the repulsive wall of the intermolecular potential. It may be possible to draw from the experiment some information about this part of the potential by using the elegant high energy analysis of F. T. Smith et al.[8] The scattering is primarily inelastic in the 20°-50° region, however, so to apply the theory it is necessary to assume that all collisions of a given impact parameter will scatter into the same center of mass angle, whether elastic or inelastic. It is by no means clear that this assumption is valid for all inelastic processes, and consequently no detailed analysis of the data of Fig. 2 has been made.

SUMMARY

This study of the dynamics of the reactions of N_2^+ with CH_4 and CD_4 has shown that over a wide range of energies, the most probable reactive event is abstraction of a hydrogen or deuterium atom by the stripping process. Although very little or no momentum is imparted to the methyl radical in such collisions, it is left with a substantial amount of internal

energy, particularly when the projectile energy is large. Even for the highest projectile energies, there is no appreciable forward recoil of the N_2H^+, in contrast to what was found in the N_2^+ - H_2, D_2, and HD systems. Even in the relatively small range of angles where reactive scattering could be detected, Q was found to be a function of angle, with product internal excitation increasing with increasing angle. The nonreactive scattering was very weak at low projectile energies, because of competition with reactive scattering. The disappearance of nonreactive scattering at all energies for angles greater than 30° indicates that small impact parameter collisions are overwhelmingly reactive or highly inelastic and spread the products very thinly over a large region of velocity space. At high projectile energies the nonreactive scattering is very inelastic, and there exists at $\theta = 0°$ and $Q = -8.2$ eV a feature which may be due to the electronic excitation of methane or of N_2^+. A very large isotope effect is observed in the reactive scattering, with the N_2D^+ product of much lower intensity and confined to smaller angles than the N_2H^+ ion. Finally, it has been demonstrated that even at what might be considered by chemists to be enormous relative collision energies, a simple abstraction reaction occurs with large cross section.

Acknowledgement: This work was supported by the U. S. Atomic Energy Commission. E.A.G. wishes to acknowledge a postdoctoral fellowship from the National Center for Air Pollution Control, Public Health Service.

Table I

Scattering Data for Reactive N_2^+-CH_4,CD_4 Collisions.

E^o(eV)	E^o_{rel}	v/v_o [a]	Q(eV)	$I(\theta=0)$ [b]	σ [c]	$I(\theta=0)$ $(Q \geq -4.7)$	σ $(Q \geq -4.7)$
				CH_4			
25.0	9.1	0.961	-1.1	89.4	5.85	89.1	5.85
45.1	16.4	0.958	-2.2	41.1	--	41.1	--
55.2	20.1	0.964	-2.1	44.9	2.58	43.9	2.11
60.2	21.9	0.958	-2.9	8.81	--	8.81	--
75.1	27.3	0.963	-2.9	10.5	1.71	9.42	0.875
75.2	27.4	0.961	-3.2	21.6	2.27	19.4	1.63
90.1	32.8	0.965	-3.2	3.91	--	3.04	--
110.0	40.0	0.969	-3.0	3.48	--	2.14	--
110.1	40.0	0.965	-3.8	2.97	0.821	1.46	0.272
130.1	47.3	0.967	-4.0	--	--	--	--
				CD_4			
25.1	10.5	0.928	-2.0	11.8	0.457	11.8	0.462
40.0	16.7	0.934	-2.6	7.97	--	7.93	--
50.0	20.8	0.937	-3.0	1.82	0.0765	1.81	0.0724
60.0	25.0	0.930	-4.4	--	--	--	--

a. The ratio of final product to initial projectile laboratory velocities.

b. Units of $Å^2$/steradian.

c. Units are $Å^2$.

References

1. L. Doverspike, R. Champion, and T. Bailey, J. Chem. Phys. 45, 4385 (1966).
2. Z. Herman, J. Kerstetter, T. Rose, and R. Wolfgang, Disc. Faraday Soc. 44, 123 (1967).
3. W. R. Gentry, E. A. Gislason, Y. T. Lee, B. H. Mahan, and C. W. Tsao, Disc. Faraday Soc. 44, 137 (1967).
4. W. R. Gentry, E. A. Gislason, B. H. Mahan, and C. W. Tsao, J. Chem. Phys. (in press).
5. W. A. Chupka, J. Chem. Phys. 48, 2337 (1968).
6. B. H. Mahan, Accounts of Chemical Research 1, 217 (1968).
7. B. R. Turner, M. A. Fineman, and R. F. Stebbings, J. Chem. Phys. 42, 4088 (1965).
8. F. T. Smith, R. P. Marchi, and K. G. Dedrick, Phys. Rev. 150, 79 (1966).

Figure 1. Velocity vector diagram for the collision of 25 eV N_2^+ with CH_4 at 300°K. The large circle is the locus of final velocity vectors for elastically scattered N_2^+, and the radius of the small circle is equal to the rms speed of CH_4. The small cross marks the velocity of N_2H^+ formed by the ideal stripping mechanism.

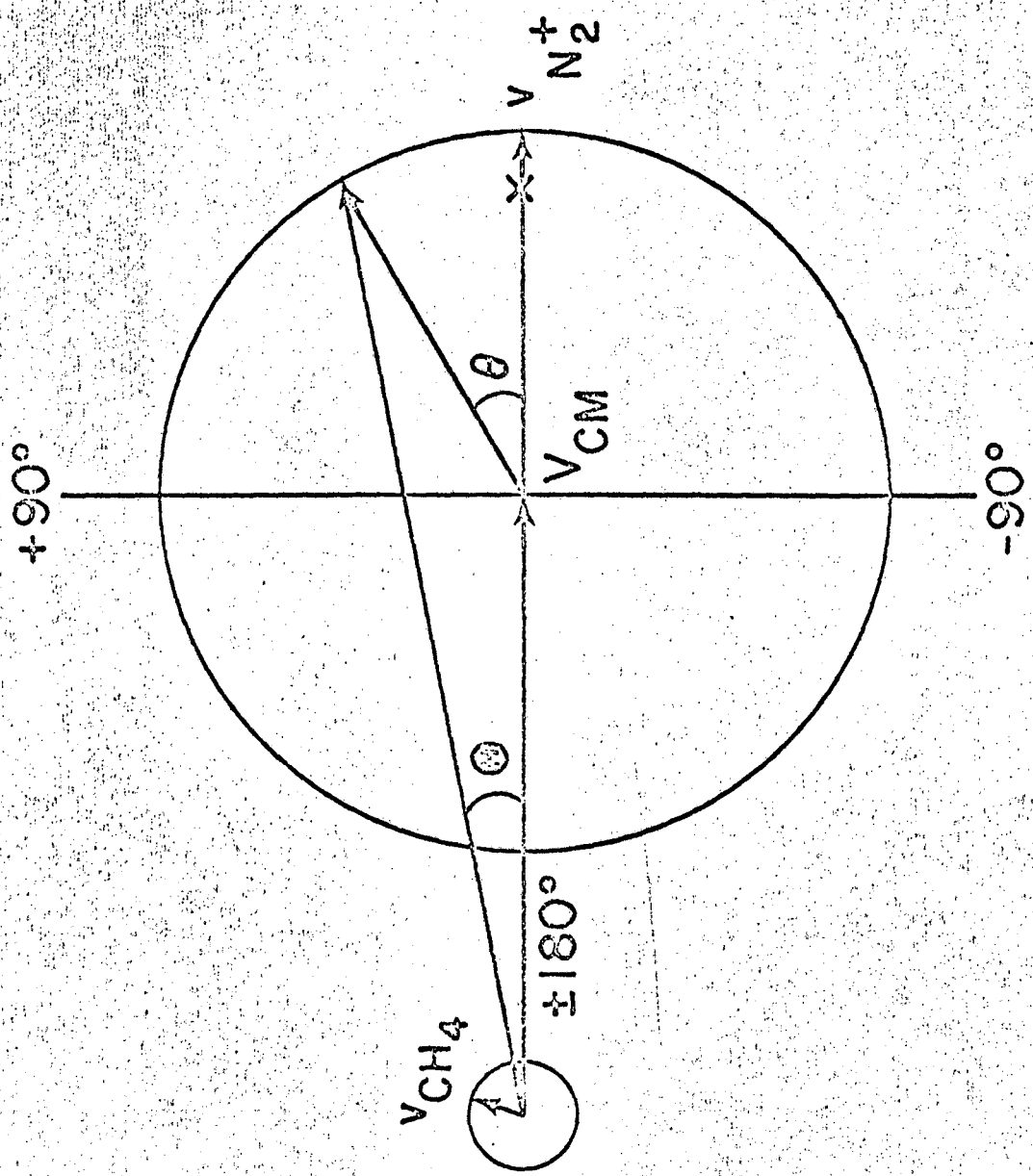
+90°
-90°
±180°
$v_{N_2^+}$
v_{CM}
v_{CH_4}
θ
Θ

Figure 2. The normalized scattered intensity of N_2^+ per unit velocity space volume in the center of mass system. The circle labeled Q = 0 is the locus of elastically scattered N_2^+. Notice how the scattering becomes more inelastic as the scattering angle increases.

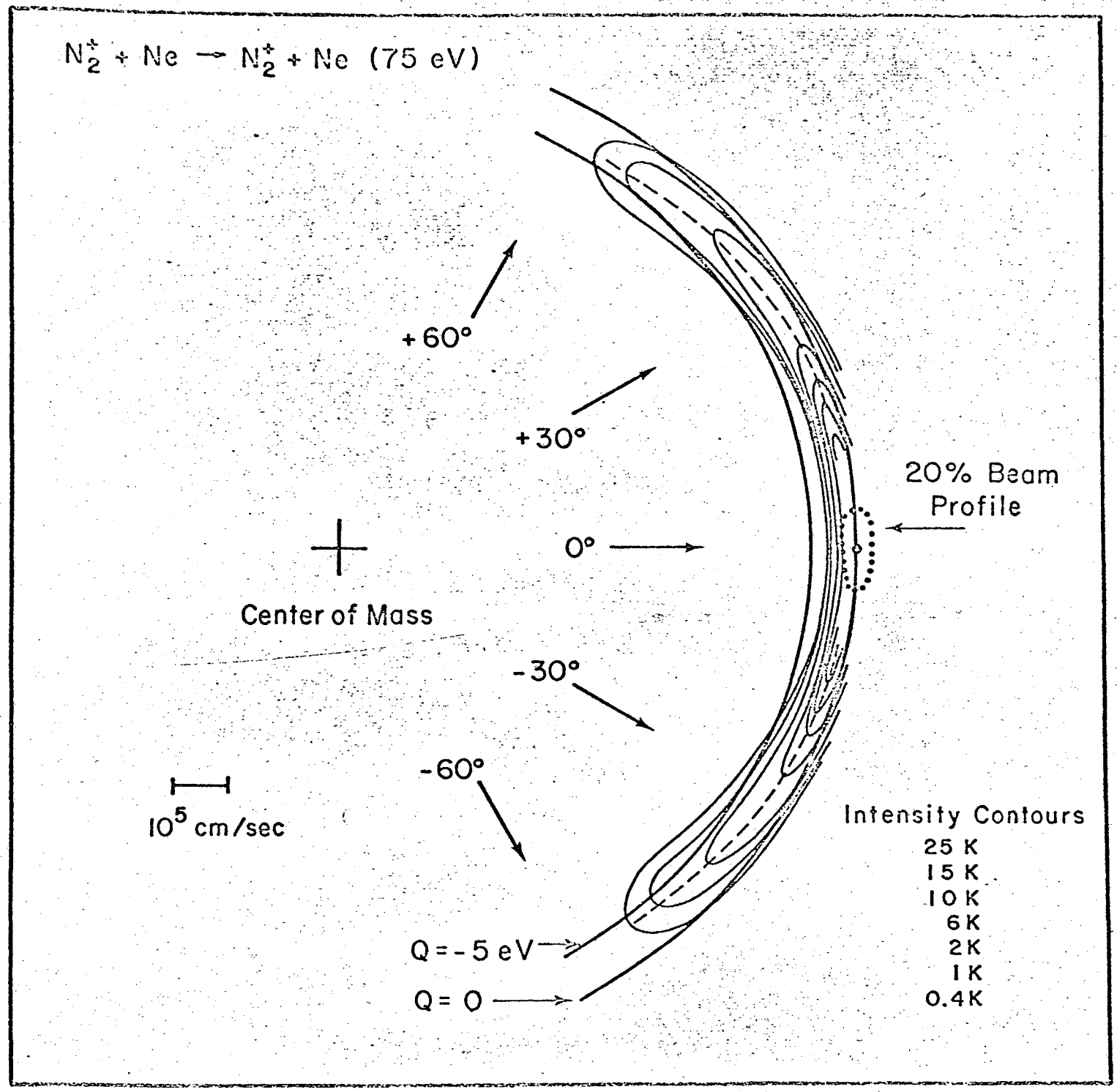
$N_2^+ + Ne \rightarrow N_2^+ + Ne$ (75 eV)
+60°
+30°
0°
-30°
-60°
Center of Mass
10^5 cm/sec
20% Beam Profile
Intensity Contours
25 K
15 K
10 K
6 K
2 K
1 K
0.4 K
Q = -5 eV
Q = 0

Figure 3. A contour map of the intensity of N_2H^+ from 25 eV N_2^+ on CH_4. The stripping velocity is indicated by a cross. Note that there is very little forward recoil, and that the Q at maximum intensity decreases and product internal excitation increases as the scattering angle increases.

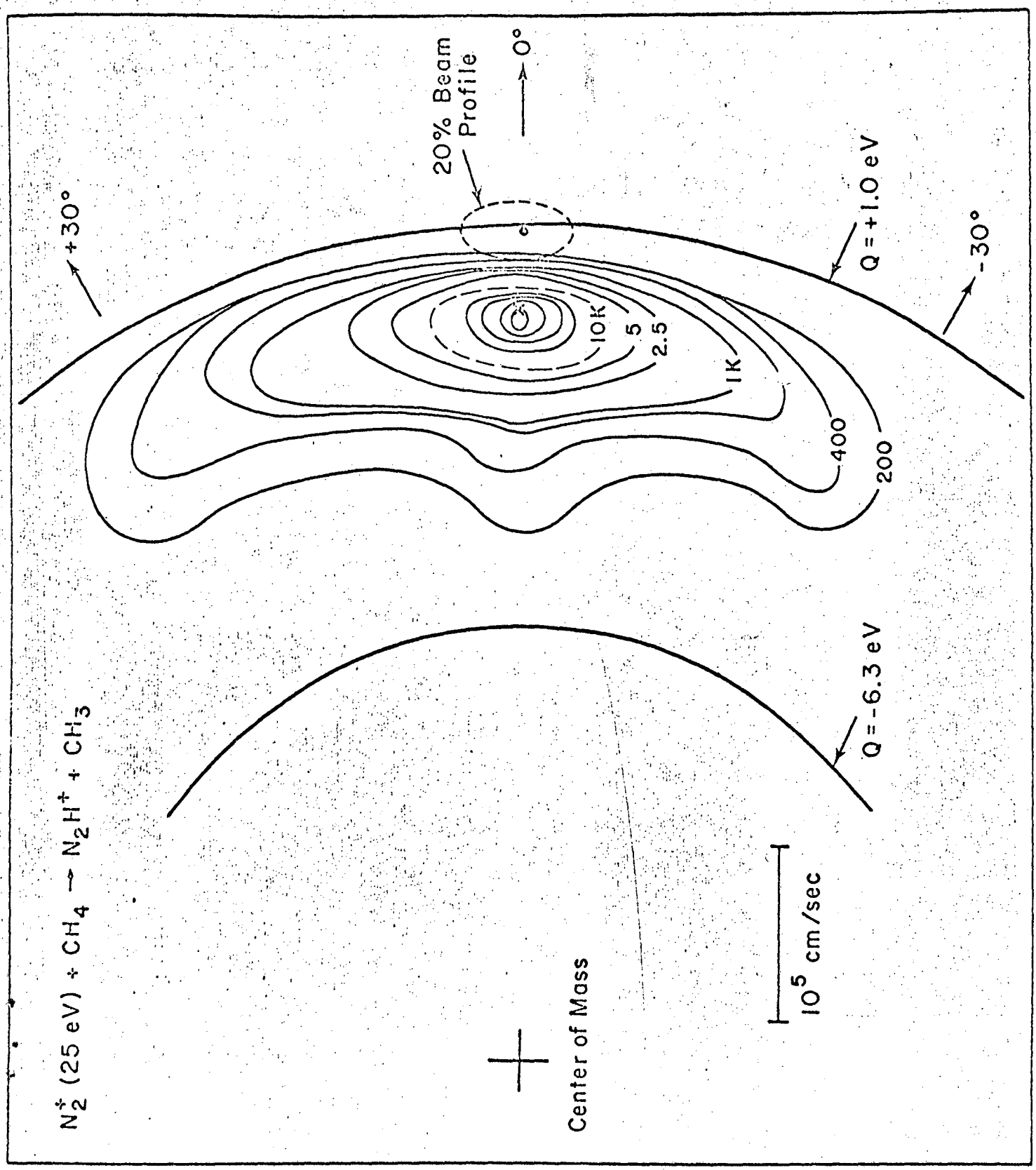
N_2^+ (25 eV) + CH_4 → N_2H^+ + CH_3
+30°
20% Beam Profile
0°
Q = +1.0 eV
-30°
10K
5
2.5
1K
400
200
Q = -6.3 eV
Center of Mass
10^5 cm/sec

Figure 4. A contour map of the nonreactively scattered N_2^+ from CH_4.

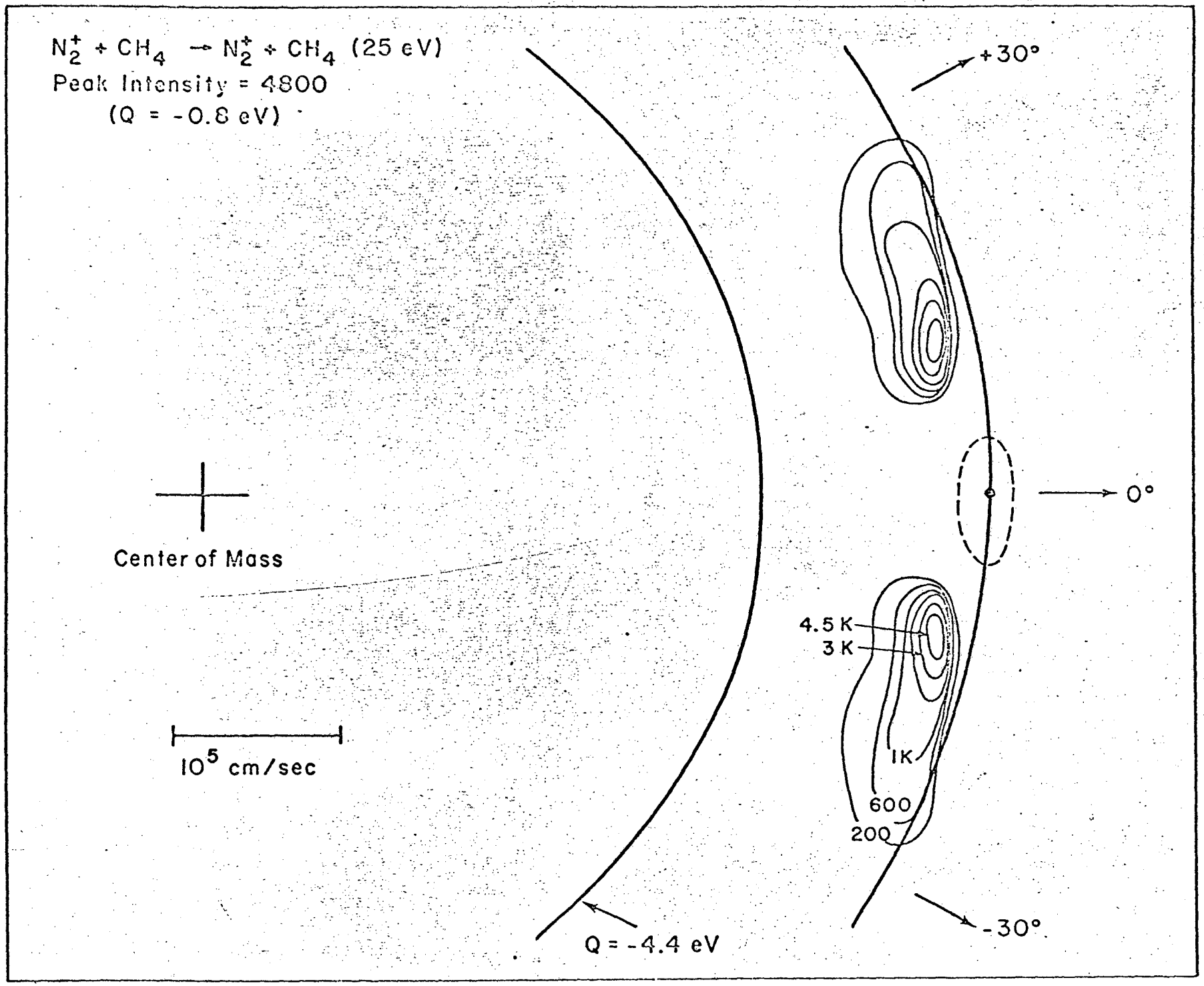
$N_2^+ + CH_4 \rightarrow N_2^+ + CH_4$ (25 eV)
Peak Intensity = 4800
(Q = -0.8 eV)
+30°
0°
-30°
Center of Mass
10^5 cm/sec
4.5 K
3 K
1K
600
200
Q = -4.4 eV

Figure 5. A contour map of the intensity of N_2D^+ from 25 eV N_2^+ on CD_4. The cross locates the velocity of N_2D^+ formed by the ideal stripping process.

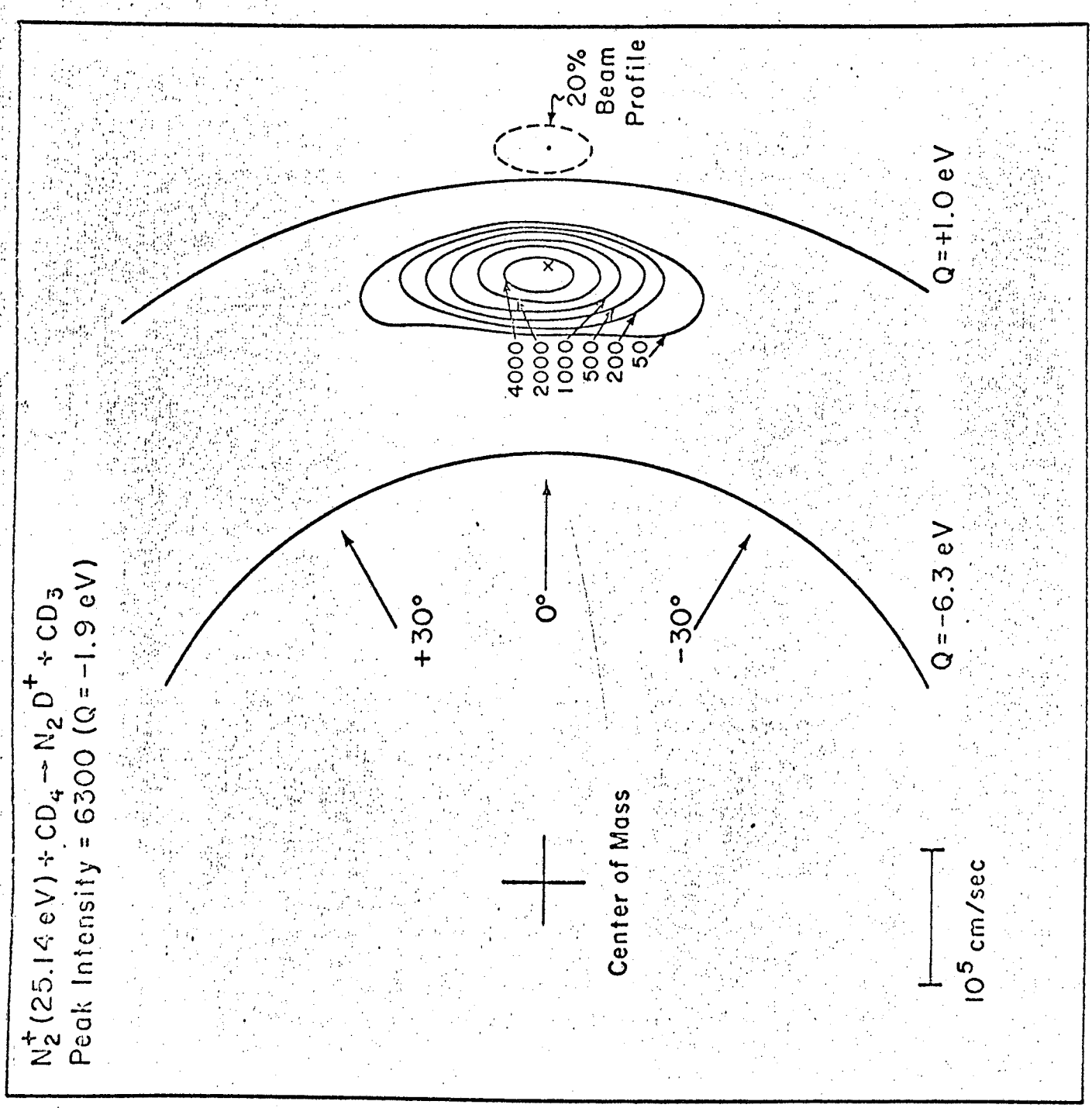
$N_2^+(25.14\ eV) + CD_4 \rightarrow N_2D^+ + CD_3$
Peak Intensity = 6300 (Q = -1.9 eV)
+30°
0°
-30°
Center of Mass
10^5 cm/sec
Q = -6.3 eV
4000
2000
1000
500
200
50
20% Beam Profile
Q = +1.0 eV

Figure 6. The intensity contours of N_2^+ scattered nonreactively from CD_4. Notice that the scattering in principally inelastic even at angles as small as 10°.

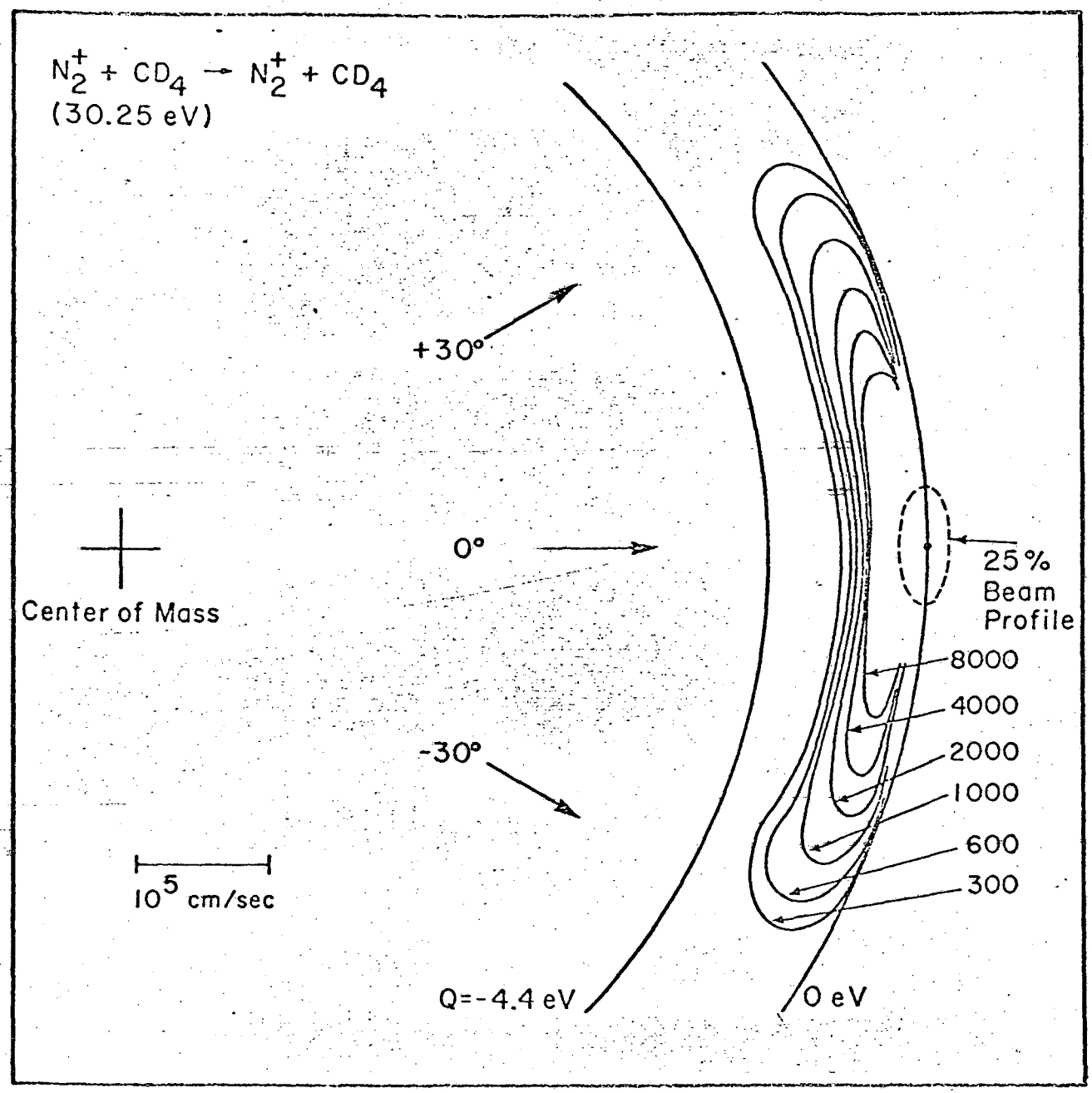
$N_2^+ + CD_4 \rightarrow N_2^+ + CD_4$
(30.25 eV)
+30°
0°
-30°
Center of Mass
10^5 cm/sec
Q=-4.4 eV
0 eV
25% Beam Profile
8000
4000
2000
1000
600
300

Figure 7. The intensity contours of N_2H^+ from 110 eV N_2^+ on CH_4. The peak intensity lies very close to the ideal stripping velocity, which is indicated by a cross. Notice that there is virtually no forward recoil, especially at small angles.

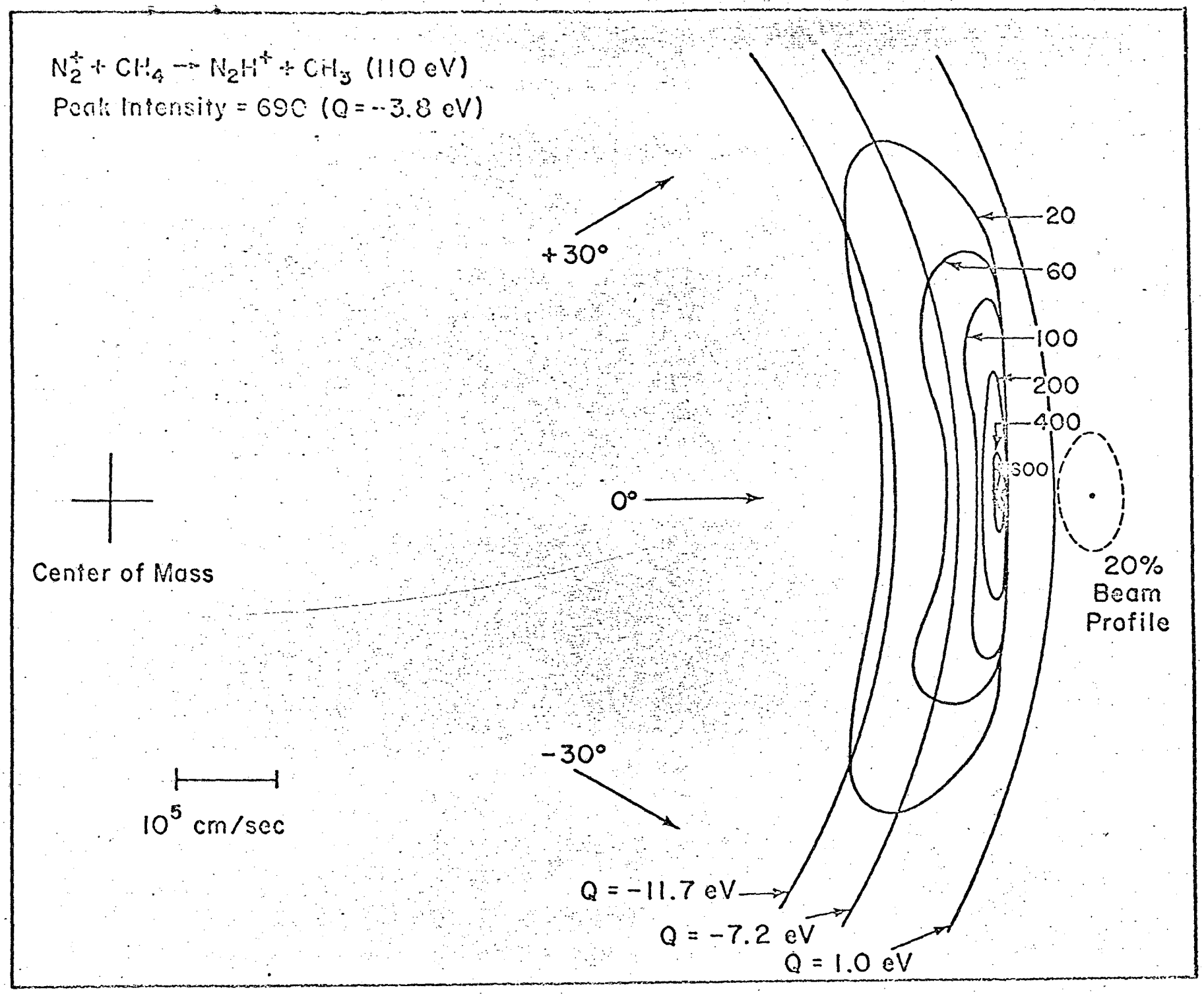
$N_2^+ + CH_4 \rightarrow N_2H^+ + CH_3$ (110 eV)
Peak Intensity = 690 (Q = -3.8 eV)
+30°
0°
-30°
Center of Mass
10^5 cm/sec
20
60
100
200
400
800
20% Beam Profile
Q = -11.7 eV
Q = -7.2 eV
Q = 1.0 eV

Figure 8. A contour map of the intensity of nonreactively scattered N_2^+. Virtually all the detected scattering is inelastic. The subsidiary maximum at Q = -8.2 and zero degrees may be due to electronic excitation of methane or of N_2^+.

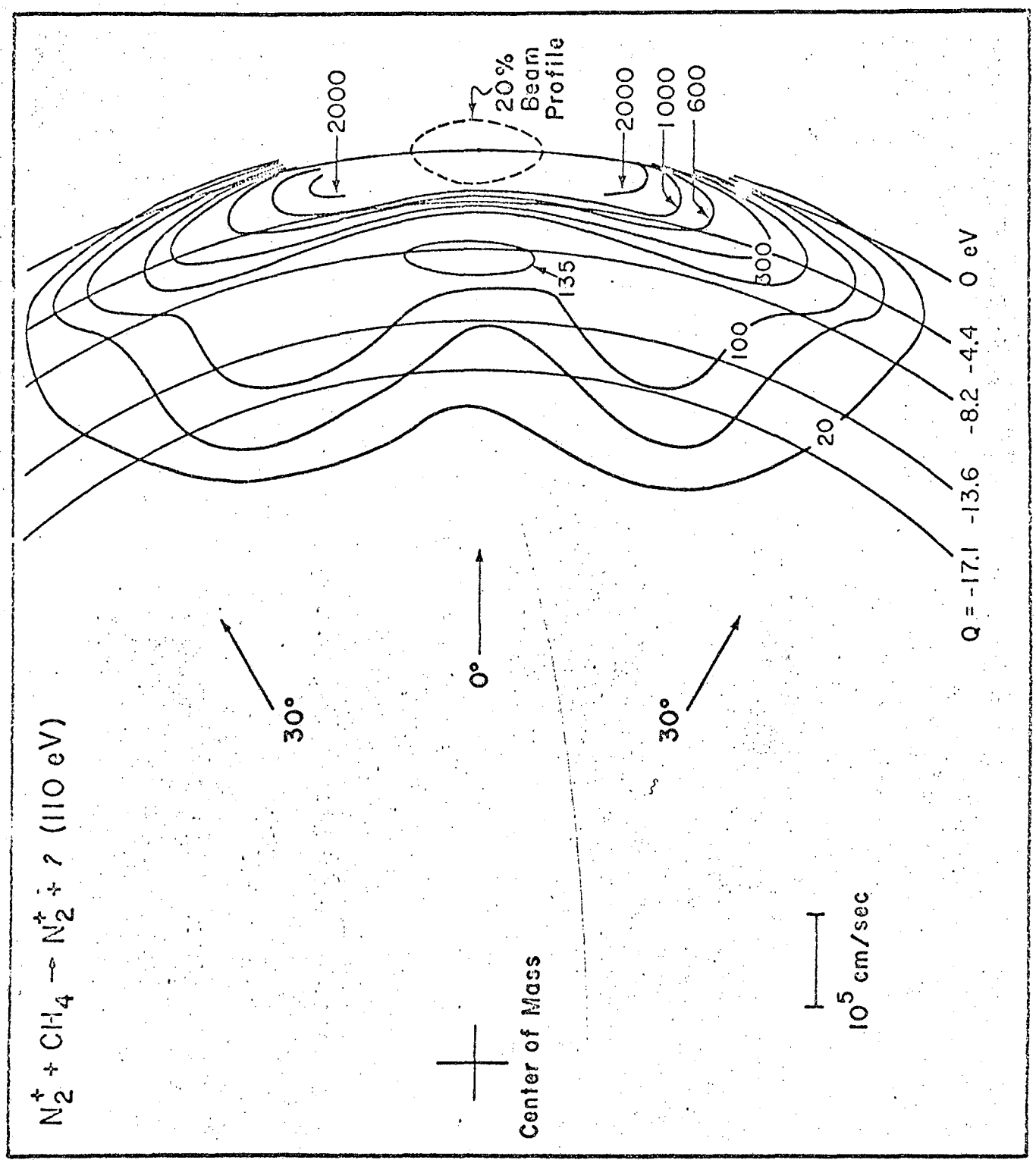
$N_2^+ + CH_4 \rightarrow N_2^+ + ?$ (110 eV)
30°
0°
30°
Center of Mass
10^5 cm/sec
2000
20% Beam Profile
2000
1000
600
135
300
100
20
Q = -17.1 -13.6 -8.2 -4.4 0 eV

Figure 9. The ratio of differential cross sections $I(\theta)/I(0)$ for formation of N_2H^+ and N_2D^+ as a function of the center of mass scattering angle θ. The labels on the curves give the values of E_a^o, the energy of the projectile relative to the abstracted atom.

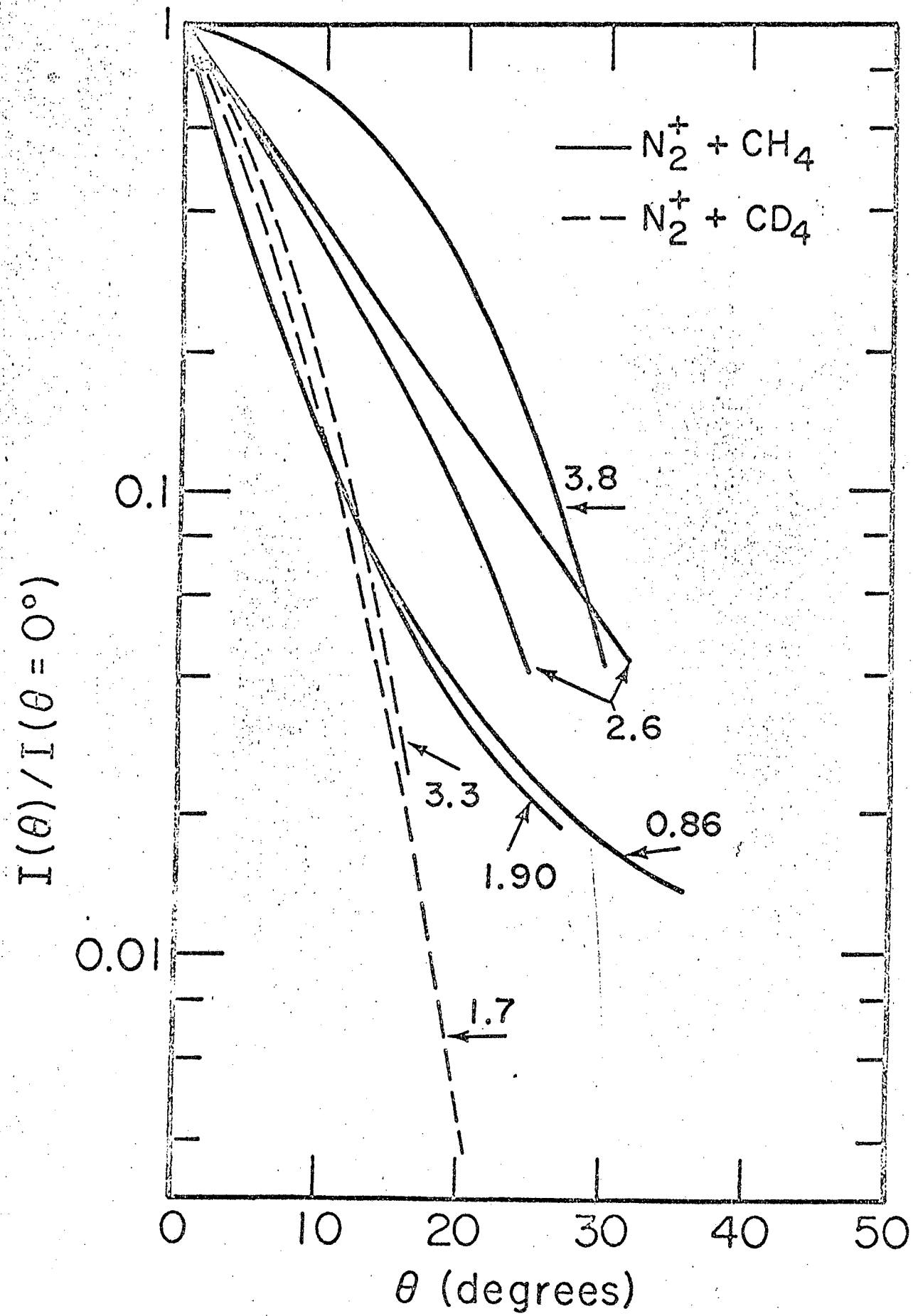
1
0.1
0.01
$I(\theta)/I(\theta = 0°)$
0
10
20
30
40
50
θ (degrees)
$N_2^+ + CH_4$
$N_2^+ + CD_4$
3.8
2.6
3.3
0.86
1.90
1.7

Figure 10. The total detected reactive cross sections as a function of E_a^o. The solid line gives the results for the reaction of N_2^+ with isotopic hydrogen molecules.

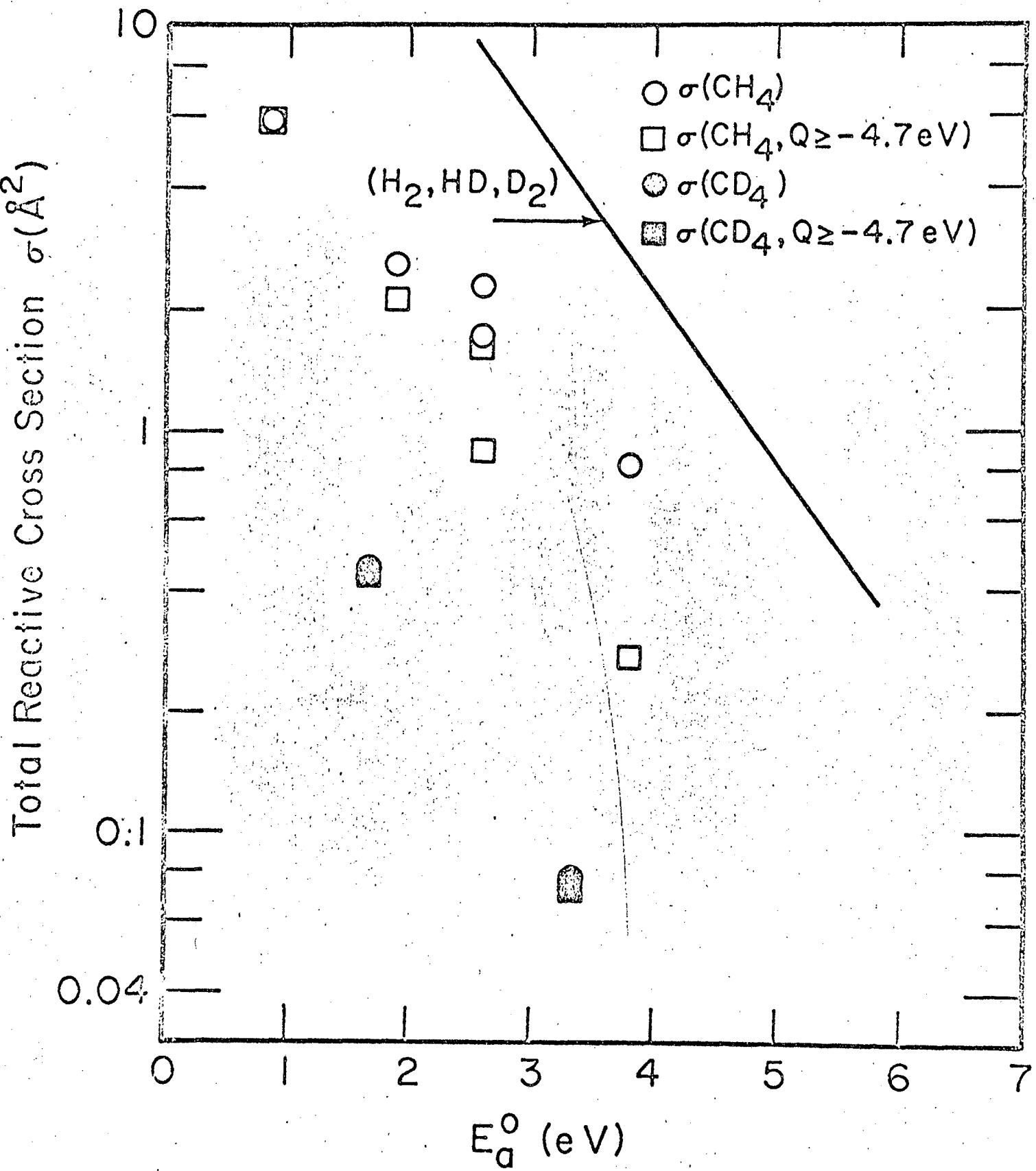
10
1
0.1
0.04
Total Reactive Cross Section σ(Å²)
0
1
2
3
4
5
6
7
E°a (eV)
(H2, HD, D2)
σ(CH4)
σ(CH4, Q≥-4.7eV)
σ(CD4)
σ(CD4, Q≥-4.7eV)

This report was prepared as an account of Government sponsored work. Neither the United States, nor the Commission, nor any person acting on behalf of the Commission:

A. Makes any warranty or representation, expressed or implied, with respect to the accuracy, completeness, or usefulness of the information contained in this report, or that the use of any information, apparatus, method, or process disclosed in this report may not infringe privately owned rights; or

B. Assumes any liabilities with respect to the use of, or for damages resulting from the use of any information, apparatus, method, or process disclosed in this report.

As used in the above, "person acting on behalf of the Commission" includes any employee or contractor of the Commission, or employee of such contractor, to the extent that such employee or contractor of the Commission, or employee of such contractor prepares, disseminates, or provides access to, any information pursuant to his employment or contract with the Commission, or his employment with such contractor.